IEEE Access
Multidisciplinary | Rapid Review | Open Access Journal

Received September 2, 2019, accepted September 24, 2019, date of publication October 7, 2019, date of current version October 23, 2019.

Digital Object Identifier 10.1109/ACCESS.2019.2945821

Research on the Air Traffic Flow Prediction Using a Deep Learning Approach

HONG LIU, YI LIN, ZHENGMAO CHEN, DONGYUE GUO, JIANWEI ZHANG, AND HAILONG JING

National Key Laboratory of Fundamental Science on Synthetic Vision, College of Computer Science, Sichuan University, Chengdu 610000, China

Corresponding author: Yi Lin (yilin@scu.edu.cn)

This work was supported in part by the Sichuan Scientific and Technological Transformative Project under Grant 2017CC0004, in part by the Key Scientific Research of Artificial Intelligence of Sichuan under Grant 2018GZDZX0029, and in part by the National Natural Science Foundation of China under Grant U1833115.

ABSTRACT In order to improve the accuracy and robustness of the air traffic prediction, in this paper, a recurrent 3D convolutional neural network (R-3DCNN) based model is proposed to consider the spatial and temporal air traffic transitions comprehensively. A new data representation, i.e., traffic situation graphics (TSG), is firstly proposed to illustrate the traffic flow situations in a single instant. A TSG is generated by splitting the 3D earth space with fixed grid map and flight levels. Motivated by the applications of deep neural network, the 3D CNN and long short-term memory (LSTM) blocks are introduced to extract high-level features (spatial and temporal) from an TSG sequence. The proposed TSG also allows us to consider some real-time factors to enrich the input information. Thus, the model input is determined by combining the traffic situations on different flight levels with areas affected by other real-time factors, such as the adverse weathers, important activities and general aviation flights. The model output is the traffic flow on different flight levels for studied airspaces at next prediction instant. The busiest routes in China are used to conduct evaluation experiments. To determine the influence of temporal dependencies, the length of input sequence is set to 30, 60 and 90 minutes before the prediction instant to select optimal architecture of the proposed model. By evaluating the prediction results with three statistical factors, we can draw the conclusion that the proposed model can obtain accurate and stable prediction results of air traffic flow with distribution on different flight levels.

INDEX TERMS Air traffic flow, flight level, recurrent 3D convolutional neural network, spatial and temporal dependency, traffic situation graphic.

I. INTRODUCTION

An accurate and prompt traffic flow prediction plays a key role in making the decisions of the passenger traveling, the concerned management measure and the governmental development plan. It also helps the air traffic controller to make more efficient and effective controlling decisions. Therefore, those purposes, relieving the air traffic congestion, reducing the exhaust gas emission, and promoting the air traffic operational efficiency, are supposed to be achieved based on the air traffic prediction [1]. Over past few years, economic achievements in China have greatly promoted the development of civil aviation transportation industry. Increasingly busy air traffic caused serious airspace resource shortage, which further results in the flight congestion and delay in busy areas. In order to solve the facing problems of civil aviation transportation in China, there is an urgent need to develop more effectiveness and efficient measures to plan and utilize the limited airspace resources. Advanced air traffic flow management (ATFM) measures are then developed to improve the flight safety and operational efficiency of air traffic system. Air traffic flow prediction (ATFP), as the core technique of the ATFM, has always been a hot research topic and attracted more and more attentions from all over the world.

In existing works of ground transportation system, the traffic flow prediction has been highly developed with advanced information technology. However, studies in air traffic system

The associate editor coordinating the review of this manuscript and approving it for publication was Ramesh Babu N.

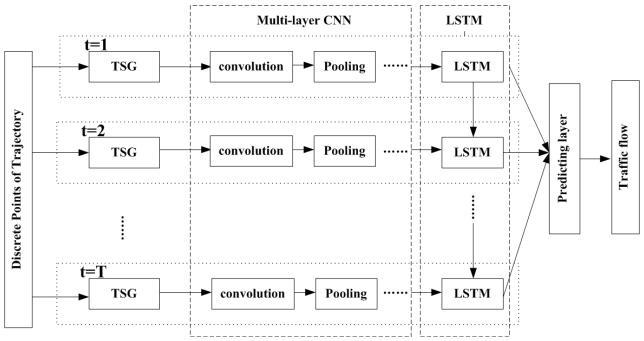

FIGURE 1. Architecture of the proposed prediction model.

did not keep up with the latest progress of algorithms and models due to safety issues. Air traffic related works preferred to simplify the computation model to ensure system stability, which usually only deals with static data without considering real time factors, such as bad weathers, important activities, military and general aviation.

Motivated by the excellent performance of deep neural network (DNN) on modeling complicated nonlinear features, we propose a deep learning-based approach to predict the air traffic flow for certain airspaces in the coming week. As a common sense, traffic patterns in an airspace are influenced by the spatial and temporal dependencies of traffic situation. Basically, the spatial dependencies come from the traffic flow in its adjacent areas. Flights in adjacent areas may locate in the studied airspace or its adjacent areas in the future according to their flight heading. Meanwhile, the traffic flow in the studied airspace is also affected by its past traffic situations, i.e., the temporal dependencies of traffic flow. Flights may stay in current airspace or fly to its adjacent areas in the future. Furthermore, flights are operated weekly based on their schedules, which also provides long-term temporal information for the ATFP research. As shown in the proposed model, the design of predicting traffic flow in next week is also based on this specificity. It can be seen that the spatial and temporal dependencies should be considered and cannot be separated in the air traffic prediction.

The most common deep leaning application of modeling spatial and temporal dependency are computer vision and natural language processing, respectively. Deep neural network (DNN) was proposed to deal with the mentioned dependencies by building the nonlinear mapping between neuros as a hierarchical architecture. Specifically, the convolutional neural network (CNN) and recurrent neural network (RNN) are designed to consider the spatial and temporal dependencies of air traffic flow, respectively. Moreover, DNNs have been introduced to the existing works on ground transportation system, which inspires us to reconsider the implementation of the air traffic flow prediction. By combining the common CNN block with 3D specificity of air traffic system, a recurrent 3D convolutional neural network (R-3DCNN) based model is proposed in this paper to predict the air traffic flow.

The general architecture of the proposed model is illustrated in Fig.1. The basic idea of this model is to consider the spatial and temporal dependencies of air traffic system comprehensively by using a new data representation, i.e., traffic situation graphics (TSG). The TSG is generated from raw flight trajectory that is a time series with discrete flight positions. A TSG has the ability of representing the spatial dependencies on adjacent areas and flight levels. The temporal dependencies of traffic flow are considered by a TSG sequence from previous instants, i.e., with a proper look-ahead prediction horizon. Based on the core idea of ATFP, the proposed model designs multiple 3D-CNN hidden layers to mine the spatial dependencies among adjacent airspaces and flight levels. Similarly, an improved RNN layer, long short-term memory (LSTM), is designed to build the temporal correlations among continuous prediction instants, in which the look-ahead horizon of the prediction model is denoted by an input TSG sequence. In short, the processing flow of the proposed model can be summarized as follows: the 3D-CNN layers encode the spatial features of the traffic situation into a vector, while the LSTM layer mines the influence of past historical traffic situations on that of current instant to predict the future air traffic flow.

Traditionally, the data-source of the prediction model would be extracted from discrete points of flight trajectory stored in a distributed database, i.e., the flight number in the studied airspaces. However, the total amount of flights in a studied area is changing all the time. More importantly, the basic deep neural network-based approaches failed to describe spatial dependencies of the air traffic flow fully for the studied airspaces in a proper form. The regression models are designed for certain airspaces based on past traffic situations, which ignored the spatial dependencies of traffic flow with adjacent airspaces. In summary, existing ATFP models failed to mine spatial and temporal dependencies of air traffic flow comprehensively, which is what we strive to achieve in this work.

In order to overcome above shortages and unify the input format (spatial and temporal dependencies) into an integrated framework, we first propose a special data representation called traffic situation graphics (TSG). A TSG illustrates the whole flight positions in the studied airspace at an updating instant. Besides, areas affected by weathers, activities and other events are also illustrated on the TSG to provide the real-time factors. An TSG splits the studied airspace into different customized airspace in the horizontal and vertical plane, which represent more dedicated extents compared to existing designed ones. The TSG also shows the overall traffic flow distributions of the studied airspace in a single data. The 3D-CNN layers are applied to extract spatial dependencies of adjacent areas and flight levels in one TSG. The LSTM layer processes temporal correlations of air traffic situation among past predicting instants. In this way, the spatial and temporal dependencies of air traffic flow are considered in the proposed model jointly. The output of the proposed model is the traffic flow of studied airspaces at next prediction instants. In addition, considering the 3D specificity of air traffic system, we further subdivide the traffic flow

into different flight levels that are designed by civil aviation administration of China (CAAC). With the consideration of spatial dependencies on adjacent flight levels, the traffic flow distribution on flight levels are predicted to further support the ATFM. For instance, based on the subdivided traffic flow distribution on flight levels, more feasible ATFM measures are supposed to be fulfilled. The most classical one is the flight level adjustment based on the 3D features of air traffic system. After analyzing the basic components in the proposed model, we design several experiments to optimize the length of input TSG sequence, i.e., the look-ahead horizon of the prediction model, the architecture of the neural network and other training hyper parameters. Experimental results on real operating data show that the proposed model can obtained more accurate and stable results over other existing approaches. The proposed model also illustrates the overall traffic flow with flight level distribution, which improves the level of the ATFP. Compared with existing prediction models, the proposed model takes both the temporal and spatial dependencies of air traffic flow into consideration, which naturally encloses sufficient traffic characteristics to improve the prediction performance. Moreover, the complicated nonlinear mapping of hierarchical architecture in a neural network manages to represent the transition patterns of air traffic flow. All in all, our original contributions in this paper are summarized below:

a) A special data representation called TSG is proposed to illustrate the spatial features of air traffic system at a single instant. The spatial correlations of adjacent horizontal regions and flight levels are illustrated on the TSG, which allows us to consider the spatial dependencies in a global level with different scale. The proposed TSG can unify spatial dependencies of air traffic flow and serves as the input of the proposed model.
b) A deep learning model based on the 3D-CNN and LSTM (an improved RNN block) is proposed to predict the air traffic flow. The 3D-CNN and LSTM blocks are designed to mine the spatial and temporal dependencies of air traffic system with complicated nonlinearity, respectively. In order to further depict the spatial dependency among different flight levels, we extend the CNN to 3D-CNN to improve the overall performance of the prediction model.
c) Instead of predicting the total flow of the studied airspaces only, the proposed TSG allows us to obtain the traffic flow for the customized and dedicated airspaces, which improve the granularity of air traffic flow and ATM measures.
d) The proposed model is able to predict the traffic flow distribution on each flight level, which greatly increases available ATFM measures and promotes the efficiency of measures.

The rest of this paper is organized as follows. Related works about this research are reviewed in Section II. Details of our proposed model are introduced in Section III. The implementations of the model training are summarized in Section IV. Section V lists the experimental configurations, design and evaluation factors. Moreover, experimental results are also reported and discussed in this section. Conclusions are in Section VI.

II. RELATED WORKS

In recent years, traffic flow prediction has been attracted more attention of researchers all over the world, and many outstanding research outcomes were achieved in this field. Existing methods of traffic flow prediction are categorized into the following groups: 4-stages prediction, stochastic probabilistic model and artificial neural network. With successful applications of deep learning (DL) on computer vision and automatic speech recognition, deep neural network-based methods were also introduced to solve present problems in the transportation research. Since air traffic is an extension of the ground transportation system, those works are of great significance to the study of air traffic system. In early 1970s, the publication of ''Chicago Area Transportation Study'' worked on the long-term traffic planning theory and method, which includes the trip generation, trip distribution, traffic mode split and traffic assignment [2]. The method played an important role in supporting the road traffic planning and urban construction. Ko *et al.* [3] proposed a method to predict the ground traffic flow by analyzing the historical trajectories and their geometric correlations. In [4], authors presented an on-line sequential extreme learning machine (ELM) model by considering historical datasets and transportation dynamics. Moreover, the model can be updated adaptively by correcting with real-time trajectories. Shang et al. proposed a short-term traffic flow prediction model named SSA-KELM (singular spectrum analysis-kernel extreme learning machine) to reduce the influence of uncertainty and nonlinearity on the expressway system [5]. An ARIMA-GARCH based model was proposed [6] to predict the short-time traffic flow. Authors integrated the ARIMA with generalized autoregressive conditional heteroscedasticity to capture both the conditional mean and heteroscedasticity of traffic flow series. Pascale and Nicoli used an adaptive Bayesian network to achieve the traffic flow prediction in [7]. They created the spatial-temporal traffic evolution graphics which is further modeled by a Bayesian network. Castro-Neto *et al.* [8] presented an online support vector machine for regression (OL-SVR) method to predict short-term traffic flow. Lv et al. introduced a deep learning approach to predict traffic flow in the next week [9], in which the neural network consists of multiple stacked auto-encoder (SAE) layers, and was trained by the greedy layer-wise algorithm. In a conference book named ''Intelligent Transportation Systems - Problems and Perspectives'', authors believed that the artificial neural network (ANN) would be a promising way to solve dozens of problems on intelligent transportation systems [10].

As to the air traffic flow prediction, Cui et al. proposed an ANN and regression combined method to forecast the air traffic flow [11]. They selected an empirical neural network

architecture and simplified some key impacts to predict air traffic flow with a rough level. Zhang proposed an ANN and double gravity model to predict air traffic flow [12]. An air traffic flow prediction algorithm called GA-WNN was proposed in [13]. Genetic algorithm was explored to optimize the wavelet neural network for the ATFP. A flight assignment method (a subtask of the ATFP) was studied by creating a dynamic system optimum (DSO) route network [14]. In [15], as a part of air traffic management, an optimization approach for the fairness and collaboration was presented to improve the air traffic operational efficiency. In [16], authors studied a subsequent topic of the ATFP called en-route, and proposed an optimized flight schedules and advanced scheduling strategy based on the traffic prediction. Cheng et al. mined frequent patterns from historical trajectories to predict traffic flow in coming hours [17], which are combined with the real-time flight distribution by statistical analysis and ANN. An air traffic flow forecasting method [18] was proposed in a linked network by analyzing the arrival time of each flight from historical trajectories. The probabilistic distribution of the flight arrival time was estimated by a non-parametric method, i.e., kernel density estimation. Sun et al. proposed an approach to estimate the traffic congestion state by probabilistic theory [19], in which the k-means algorithm was used to generate traffic situation and support vector machine was applied to train a traffic model to predict the traffic jam. In [20], authors applied an analogous model to improve the air traffic monitoring and controlling of terminal areas in real-time. By classifying the terminal congestion into five levels, they forecasted the air traffic condition in busy areas to support the decision-making. The real-time operating data in the Eurocat-X system, such as flight plan, radar and automatic dependent surveillance-broadcast (ADS-B), was applied to predict the current and short-term air traffic flow in [21]. Least squares support vector regression-based prediction model was introduced in [22].

Even though the CNN and RNN combined models are new for the air traffic flow prediction, some works have been applied the neural network with similar architecture to other fields. The CNN applications concerned the image classification, object detection, etc. [23] As to its combination with RNN block or improved architectures, two-stream convolutional networks (ConvNet) were proposed to recognize actions in videos [24]. Donahue et al. developed a recurrent convolutional model called LRCNs for the large-scale visual learning [25]. Sequential 3D-CNN models for human action recognition were studied in [26] and [27]. The models extracted features from both spatial and temporal dimensions by performing 3D convolutions, and thereby captured the motion information between video frames. Lai et al. applied a recurrent architecture to capture contextual information for the text classification task [28]. CNN layers were designed to model the left context, word embedding and right context of a single word, while the recurrent architecture was used to capture the temporal relationship between words. Pinheiro et al. proposed recurrent convolutional neural networks [29] to perform the scene labeling task. The CNN and RNN were used to extract spatial features from local region and long range (pixel) label dependencies in images, respectively. Those works provide the available reference on model architecture in this work.

III. METHODOLOGIES

A. TRAFFIC SITUATION GRAPHICS

Air traffic control builds communication, navigation and surveillance infrastructures to provide basic information for nationwide air traffic system [30]. The radar network monitors and tracks flying targets in the air. Various attributions of the target can be recognized, including the aircraft identification, longitude, latitude, altitude, velocity, heading, et al. Each equipment keeps 4-seconds updating interval and sends its recognized information to a data fusion center. In order to generate discrete trajectory positions, the multi-source and multi-type data items are processed by decoding, registration, tracking and fusion algorithms [31].

As previously described, the real-time flight number in an airspace is uncertain and changing as the time elapsed. Meanwhile, the traffic flow on adjacent areas and flight levels should also be considered in the ATFP and constructed in the model input properly. Therefore, we propose a new data representation called traffic situation graphics (TSG) to integrate the traffic flow situations and build the interactive influence among all customized airspaces and flight levels. The whole 3D air traffic system is firstly split into 2D transportation scenes based on the standard flight levels designed by CAAC. In each 2D horizontal plane, the traffic is further divided into grids with fix size, in which each grid denotes a certain spatial extent. The flight number in the grid is regarded as the traffic flow. Consequently, the traffic on the 2D plane is encoded as an image whose pixel value is represented by the flight number in corresponding grids. Fig.2 shows the mappings between the TSG and real traffic situation. The altitude is split into 45 levels and arranged by a level code from 1 to 45 in a TSG. In this paper, the grid size is 20 KM * 15KM because of the width of route (typically 20 KM) and flight interval restriction (typically 15 KM) in China. Finally, the whole air traffic situation at a certain moment is constructed into a 250*250 image with 45 channels approximately. A TSG sequence with proper temporal memory serves as the input of the proposed model and is processed by the following 3D-CNN layers.

Furthermore, to illustrate the real-time flight impacts, all affected areas are also indicated in each grid. In general, the real-time factors mainly affect the dynamic capacity of related airspaces. Therefore, we imply real-time factors concerned airspace capacity to illustrate the influence. If the airspace is restricted by some events (bad weathers, traffic flow controlling, etc.), the airspace capacity will be reduced to some extent. Consequently, we increase the traffic flow in the affected areas to illustrate real-time factors, as shown in (1). l is pixel value of the cells in affected area on the

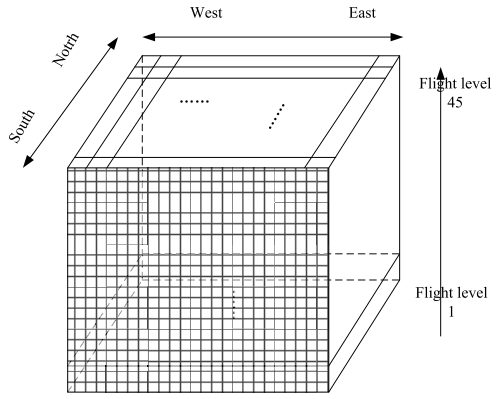

FIGURE 2. The description of nationwide traffic situation graphic.

TSG. R is the range of the gray value. V_s and V_d are the static and dynamic capacity (affected by real-time factors) respectively [32]. V_s in an airspace is evaluated and published by a top-level ATC department. V_d in an airspace is a real-time evaluation, which is determined by the low-level ATC department.

$$l = R \times \frac{V_d}{V_s} \tag{1}$$

B. CNN

CNN is a kind of neural network, which is proposed to extract high-level features of spatial dependencies, such as image. A CNN layer is usually designed with a pooling layer to mine discriminative features and compress the data dimension. The general architecture of a CNN layer is showed in Fig.3 [33]. The convolutional operation is designed to mine spatial correlations among adjacent grids on a TSG. In general, CNN designs several different convolutional kernels to extract diverse features for modeling spatial correlations. The weights among interdependent adjacent grids are shared to make the feed-forward propagation and backward training become more efficient in practice. The convolutional operation allows the CNN block to maintain the rotation, distortion and scaling invariance for spatial features, which promotes the performance of spatial modelling. For example, the traffic patterns on different routes can be captured and learned by the rotation of CNN.

$$x_j^l = f(\sum_{i \in M_j} (x_i^{l-1} * \Delta_{ij}^l) + b_j^l) \tag{2}$$

$$x_{ij}^l = g(x_\varsigma^{l-1}) \tag{3}$$

The forward inference of a CNN block is listed in (2) and (3), in which the former one is the propagation rule of a convolutional layer, and the latter one shows the formulation of a pooling layer. x_j^l is the output of j^{th} neuron in layer l. Operator $*$ denotes the convolution operation, Δ_{ij}^l is the convolutional kernel of the j^{th} neuron in layer $l$and i^{th} neuron in layer $l-1$. b_j^l is the bias of j^{th} neuron in layer l. $f(.)$is the non-linear activation function, such as sigmoid, tanh and

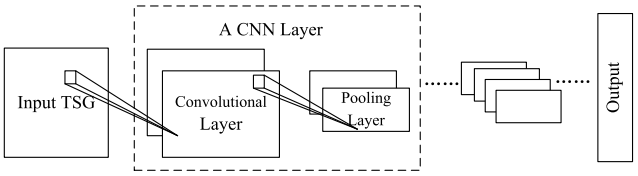

FIGURE 3. The general architecture of CNN.

ReLU (Rectified Linear Unit). ς indicates the spatial field for processing the pooling operation in layer l. $g(.)$ is the sub-sampling function in a pooling layer, which is usually specified as average, median or maximal operation.

In the ATFP, the traffic flow of an airspace is greatly influenced by other adjacent airspaces. Therefore, CNN layers are designed to mine spatial dependences of traffic flow patterns in our proposal. Moreover, due to the 3D character of air traffic system, the air traffic flow on given flight level is also interacted by the traffic situation on adjacent flight levels. Consequently, we extend the CNN operation to the 3D data space, i.e., 3D-CNN, to extract diverse features and spatial dependencies on different flight levels. Typically, the convolutional operation of the CNN can be detailly expressed as (4). Considering the 3D specificity, the inference rule for 3D-CNN are rewritten as (5). In the CNN block, deeper layers are expected to extract high-level abstract features, which is the key to mine spatial dependencies of traffic flow patterns.

$$v_{ij}^{xy} = \sum_m \sum_{p=0}^{P_i-1} \sum_{q=0}^{Q_i-1} w_{ijm}^{pq} v_{(i-1)m}^{(x+p)(y+q)} \tag{4}$$

$$v_{ij}^{xyz} = \sum_m \sum_{p=0}^{P_i-1} \sum_{q=0}^{Q_i-1} \sum_{r=0}^{R_i-1} w_{ijm}^{pqr} v_{(i-1)m}^{(x+p)(y+q)(z+r)} \tag{5}$$

In the listed equations, v is the value at a grid index (denoted by x, y, z) on the j^{th} feature map in the i^{th} layer. m saves the total number of the feature map. P_i, Q_i, R_i are the configuration of the convolutional kernel in three dimensions, respectively, i.e., the width, height, depth. w_{ijm}^{pq} and w_{ijm}^{pqr} are $(p, q)^{th}$ and $(p, q, r)^{th}$ weights of the convolutional kernel connected to the m^{th} feature map in the previous layer, respectively.

C. LSTM

LSTM is an improved RNN block, named long-short term memory, which receives not only the output of the previous layer but also the output of the last prediction instant. For each hidden unit s in an RNN block, the input comprises of the $x^{(s)}$ at current instant and the $h^{(s-1)}$ at last time instant, as shown below.

$$\begin{aligned} h^{(s)} &= f_h(w_{hh}h^{(s-1)} + w_{ih}x^{(s)} + b_h) \\ y^{(s)} &= f_o(w_{ho}h^{(s)} + b_o) \end{aligned} \tag{6}$$

In (6), $h^{(s)}$ and $y^{(s)}$ are the hidden activation and output of the hidden unit s, respectively. b_h and b_o represent the bias of

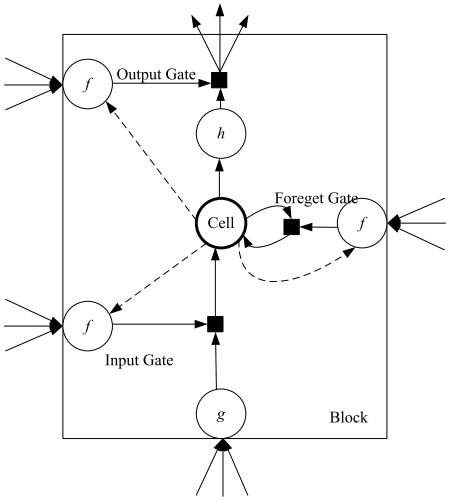

FIGURE 4. The general architecture of LSTM.

the hidden activation at last and current time instant, respectively. w_{hh}, w_{ih} and w_{ho} indicate the weights of the connection between hidden units in neighboring timestep, input units and output units of current time step, respectively. The connections of hidden units between different time instants are the key to share the sequential information of air traffic flow. However, excessive connections in the RNN block impose extra computational burdens on training progress, including gradient vanishing and exploding. The block used in this work, i.e., LSTM [34], was proposed to solve those issues. A LSTM block comprises a memory cell, and three control gates, i.e., the input, output and forget gates, as shown in Fig.4 [35]. The vectorized inference rules of the LSTM block are shown in (7). By controlling the weight of the information transmission among the three gates, the important sequential information is propagated to the next timestep to build the temporal dependencies of the input sequence. In this work, after extracting deep spatial features from TSG sequence using 3D-CNNs, temporal dependencies among historical TSGs are built by a LSTM layer.

$$\begin{aligned}
\boldsymbol{I}^t &= f(\boldsymbol{W}_{ix}\boldsymbol{x}^t + \boldsymbol{W}_{ih}\boldsymbol{h}^{t-1} + \boldsymbol{W}_{ic}\boldsymbol{C}^{t-1} + \boldsymbol{b}_i) \\
\boldsymbol{F}^t &= f(\boldsymbol{W}_{fx}\boldsymbol{x}^t + \boldsymbol{W}_{fh}\boldsymbol{h}^{t-1} + \boldsymbol{W}_{fc}\boldsymbol{C}^{t-1} + \boldsymbol{b}_f) \\
\boldsymbol{C}^t &= \boldsymbol{F}^t \circ \boldsymbol{C}^{t-1} + \boldsymbol{I}^t \circ g(\boldsymbol{W}_{cx}\boldsymbol{x}^t + \boldsymbol{W}_{ch}\boldsymbol{h}^{t-1} + \boldsymbol{b}_c) \\
\boldsymbol{O}^t &= f(\boldsymbol{W}_{ox}\boldsymbol{x}^t + \boldsymbol{W}_{oh}\boldsymbol{h}^{t-1} + \boldsymbol{W}_{oc}\boldsymbol{C}^t + \boldsymbol{b}_o) \\
\boldsymbol{h}^t &= \boldsymbol{O}^t \circ g(\boldsymbol{C}^t)
\end{aligned} \tag{7}$$

where, $\boldsymbol{I}^t$, $\boldsymbol{F}^t$, $\boldsymbol{C}^t$, $\boldsymbol{O}^t$ are the activations of the input gate, forget gate, cell, and output gate, respectively. The superscript t denote the predicting instant. $\boldsymbol{W}_{..}$ save the weight tensor, whose subscripts indicate the direction of the information transmission. For example, the subscript fh of $\boldsymbol{W}_{..}$ shows the direction from hidden unit of last time instant to forget gate at current time. $\boldsymbol{b}_{.}$ is the bias in the corresponding component.

D. D.R-3DCNN

As described before, both the whole nationwide traffic situation (spatial) and traffic situation at past time instants (temporal) should be considered in the ATFP. In this paper, a CNN- and RNN- combined neural network is designed to consider both the spatial and temporal dependencies jointly for predicting the air traffic flow. Furthermore, we extend the common CNN operation to the 3D-CNN to mine the spatial correlations among adjacent customized airspaces and flight levels integrally. To cope with the long-time dependency of the input sequence, i.e., the look-ahead horizon of the prediction model, we also apply LSTM blocks to improve the accuracy and robustness of the prediction model. The architecture of the proposed model is shown in Fig.1. The input TSG sequence is first fed to 3D-CNN to extract spatial features in horizontal plane and vertical direction at each predicting instant. The improved RNN block, i.e., LSTM, is designed to mine temporal correlations among historical TSGs. With the designed blocks, a deep neural network based ATFP approach comes into being. The architecture of the model is detailly described below:

a) The TSG is organized as a 3D data (3D dependencies), where the spatial dependencies of the air traffic flow concern the adjacent areas and flight levels. Therefore, more CNN layers are designed to extract the transition patterns of air traffic flow in the proposed model.
b) Since a TSG illustrates a global traffic situation in the studied airspaces, the spatial dependencies are reflected in different spatial scales (corresponding to different kernel size of convolutional operations), just like a pyramid architecture. That is to say, the near areas influence the traffic flow of a certain airspace in a short term, where the far areas are in a long term. This is also the reason why multiple CNN layers are needed to extract traffic flow patterns.
c) As we can see, the temporal dependencies of air traffic depend only on the traffic situation of past instants, i.e., 1-D dependencies. Moreover, the TSG represent the air traffic in more refined and dedicated customized airspaces, in which the nonlinearity of the traffic flow is easy to be captured compared to the spatial dependencies. Therefore, we only designed one LSTM layer to obtain the temporal transition patterns of air traffic.

After determining the blocks of the proposed network, the next step is to optimize the parameters of the network by an effective algorithm with large number of credible training data.

IV. MODEL TRAINING

The training of a deep learning model aims at learning the data distribution from training samples by optimizing the trainable parameters of the neural network. The difference between the true labels and predicted outputs is evaluated by a loss function. Meanwhile, a regularization item is also proposed to improve the generalization of the deep learning

model. In general, the optimization target of the model training consists of an estimation error item (J) and a regularization item (R) [36], as shown in (8).

$$\theta = \arg\min_{\theta} L(X, Y) = \arg\min_{\theta}(J + \lambda R) \tag{8}$$

$$J = -\frac{1}{m}\sum_{i=1}^{N} f(y(i), y'(i)) \tag{9}$$

In the listed equations, θ represents the parameter set of a deep neural network, including trainable weights and biases. λ denotes the hyper parameters of the regularization item. J is the loss function, and R is selected as Frobenius norm. m saves the total number of training samples. X, Y save the inputs and outputs of the model, respectively. $y(i)$ and $y'(i)$ are the true label and predicted output of the i-th training sample, respectively.

Other details of training hyper parameters are sketched below. The activation function is ReLU in this work. In order to speed up the training progress, mini-batch gradient descent with 16 samples per iteration is applied to update training parameters in the back-propagation algorithm. All parameters (weights and biases) in the proposed neural network are initialized by sampling from a uniform distribution. The updating of the weights and biases is shown in (10), in which W, b are the vectorized weight and bias tensors, respectively. Batch normalization is applied to adjust the data distribution of training samples after CNN layers. Dropout layers are used to cut some connections between nodes of two adjacent layers to prevent the over-fitting problem. The Adam optimizer is applied to improve the performance of gradient descent algorithm with 0.001 initial learning rate, 0.9 beta_1, 0.999 beta_2 and $\varepsilon = 1e-8$. The proposed network is totally trained 50 epochs with shuffling the training samples. The parameters of the proposed model, including the number of the CNN layers, the number of hidden units of each layer, the configuration of convolutional kernels, the size of subsampling kernel, and the neuron of LSTM cell, need to be determined to obtain the best prediction performance.

$$\begin{aligned} W &:= W - \alpha(\partial J/\partial W) \\ b &:= b - \alpha(\partial J/\partial b) \end{aligned} \tag{10}$$

V. EXPERIMENTS AND DISCUSSIONS

A. EXPERIMENTAL CONFIGURATIONS

Since the flight execution in China mainly follows the flight schedule published by civil aviation department, which contains a spring and autumnal version. All flights usually operate in weekly, i.e., week cyclicity [37]. The studied airspaces in this paper are the busiest routes in China, including the Beijing-Shanghai (JHR) and Beijing-Guangzhou (JGR). The primary task of the experiment is to predict the air traffic flow of the two routes with flight level distribution in next flight period (weekly). Several experiments are first designed to optimize the model architecture and parameters, such as the number of the CNN layers, the configuration of convolutional kernels, the look-ahead prediction horizon, etc. Based on an preliminary analysis of air traffic situation, three candidates serves as the option of the look-ahead horizon of the prediction model, i.e., 30, 60, 90 minutes before the predicting instant [38]. All the three options are taken part in the designed experiments to obtain a best look-ahead horizon of the prediction model. Historical trajectories of executed flights are the raw data of the proposed model and real-time affected areas are also considered in the ATFP. The raw updating interval is about 10 seconds, while the raw data is converted into the TSGs with one-minute updating interval based on fact that the traffic situation of a certain airspace in one minute is steady. Flight trajectories from December 29, 2014 to May 29, 2016 are used to generate training samples for the proposed prediction model, and the flight trajectories from May 30, 2016 to June 5, 2016 (a week) are also collected and processed for the final test in the similar way. The whole dataset is further divided into two parts, in which the training and validation set account for 95% and 5%, respectively. We also design several comparison experiments, including the flight trajectory prediction-based method (FTP) [39], the regression-based prediction model (RP) [6] and the neural network-based ones (NN). Since the proposed model is a neural network-based one, the following architectures, including the fully connected neural network (FC-NN), common recurrent neural network (B-LSTM), FC and LSTM combined (FC-NN+LSTM), 2D-CNN and LSTM (2D-CNN+LSTM) combined model, are designed to validate different improvements in this work. In this paper, all predicted results obtained by different methods are evaluated by the following three measurements:

1) Mean prediction error (MPE)

$$MPE = \frac{1}{n}\sum_{i=1}^{n}\left|f_p^i - f_c^i\right| \tag{11}$$

2) Mean error ratio (MER)

$$MER = \frac{1}{n}\sum_{i=1}^{n}\frac{\left|f_p^i - f_c^i\right|}{f_c^i} \tag{12}$$

3) Prediction error variance (PEV)

$$PEV = \sqrt{\frac{1}{n}\sum_{i=1}^{n}\left|f_p^i - f_c^i\right|^2} \tag{13}$$

where n is the total number of the predicted samples in the test data. f_p^i and f_c^i are the predicted and real value of i^{th} training samples, respectively. The first two measurements mainly focus on the accuracy of the predicted results, in which the second one is a measurement of the relative error percentage. The last one focuses on the stability and robustness of the prediction results for dealing with different traffic situations.

The main configurations of the training server are summarized as: 2*Intel Xeon E5-2650 CPUs, 64GB memory, and 2* NVIDIA GTX 1080 GPUs, and the operation system is Ubuntu 16.04. All codes are programmed using Python, and

deep learning-based model is constructed based on the open framework Keras (2.0.4) with TensorFlow (1.0.0) backend.

B. INPUT AND OUTPUT

All the raw flight trajectories are first converted into the training samples, i.e., (X, Y) pairs that represent the input and output of the neural network. In this paper, X is a TSG sequence generated by our proposed data representation. The shape of X is tuple with 6 elements, as shown below: X = (batch-size, timestep, width, height, depth, channel). The batch-size is the sample size for implementing the mini batch gradient descent algorithm. The timestep is the temporal memory of LSTM block, i.e., the look-ahead horizon of the prediction model. The width and height denote the shape of the horizontal TSGs on each flight level, 250*250 in this work. The depth is the third dimension of the TSG, namely flight level, 45 in this work. The channel is the channels of the 3-D TSG, 1 in this work. Y is the traffic flow vector for the studied airspaces in each flight level.

C. NETWORK ARCHITECTURE

The parameters concerned the model architecture comprise the number of the 3D-CNN layers, the number of hidden units of each layer, the configuration of the convolutional kernels, the size of the sub-sampling kernels, the nodes of the LSTM layer. Those parameters are determined by several designed experiments. In this paper, the input shape of the proposed neural network is (batch-size, timestep, 250, 250, 45, 1), the output is the vector with 90 dimensions, i.e., 2 (the number of the studied airspaces, JHR and JGR) multiply 45 (the number of flight levels). In this paper, the number of 3D-CNN hidden layers is selected from 3 to 6, and the size of convolutional kernel and sub-sampling must be ensuring the output dimension. The sub-sampling function is max-pooling operation. The final architecture of the proposed model will be determined by experiments in the later section.

D. RESULTS AND DISCUSSIONS

The first experiment focuses on confirming the model parameters, i.e., feeding the TSG sequence with different look-ahead horizon into the neural network with different number of 3D-CNN hidden layers to evaluate the model performance. The prediction results consist of the traffic flow of the studied airspaces and their distribution on different flight levels. All predicted traffic flow are evaluated by the proposed three measurements, i.e., MPE, MER and PEV. Experiment results in this section are reported in the Tab.1, in which the input length and #h denote the look-ahead horizon of the prediction model, and the optimal number of the hidden 3D-CNN layers, respectively.

From the results in Tab.1, we can see that:

a) Regarding the model trained by the data collected 60-minute before the prediction instant, the prediction results for both the total flow and its flight level distribution are more accurate (lower MPE and MER) and stable (lower PEV) than that of other options even using a simpler model architecture. In general, the 30-minute TSG sequence fails to provide enough temporal dependencies for the air traffic prediction, in which the transition patterns of air traffic flow are not fully implied. Consequently, more CNN layers are needed to extract the incompatible transition patterns, which turns out to limit the model performance.

b) Comparing the predicted traffic flow obtained by the TSG sequence 90-minute before the prediction instant, the results are not comparable with that of 60-minute TSG sequence, in both the accuracy and stability. If a longer historical TSG sequence is taken by the neural network, more non-determinacy flight patterns are inclined to be introduced during the model training. It turns out to be that the longer input TSG sequence not only increases the complexity of network architecture but also imposes detrimental influences on the accuracy and stability of the final results.

c) Based on the results, we find that most of the predictions obtained with 90-minute historical memory are nearly as accurate as that of 60-minute historical memory by computing the prediction error on each predicting instant. However, the remaining results fluctuate in a wide range, and they are even not comparable with the results obtained by only the 30-minute look-ahead horizon. The reason of the results can be attributed that most of the flight time are about 120-180 minutes. Due to the studied airspaces are arterial routes, flights will go through the studied airspaces in about 60 minutes. Therefore, more hidden layers are required to mine the dependency for a longer TSG sequence. Meanwhile, the prediction accuracy and stability are not promoted as expected due to the feeding of the interferential model input.

TABLE 1. Results with different input length and CNN layers.

Input length	#h	Total traffic flow			Flight level distribution		
		MPE	MER (%)	PEV	MPE	MER (%)	PEV
t-30	5	8.50	8.71	10.06	0.21	2.37	0.44
t-60	4	5.67	5.25	5.97	0.15	1.92	0.37
t-90	6	6.98	7.05	11.25	0.20	2.36	0.41

Judging from above discussions, we can see that the TSG sequence with 60-minute look-ahead horizon is a preferred option for training the proposed prediction model. With the determined look-ahead horizon, the prediction results are optimized by the neural network with 4 hidden 3D-CNN layers. For the 3D-CNN training, we select an optimal architecture for the proposed model, as listed in Tab. 2. The configurations of the convolutional and pooling kernel in each hidden layer are reported in this table. The digits after @ denote the number of filters for convolution operations, which also denotes the output depth in each hidden layer.

TABLE 2. The CNN configurations.

Layer name	Kernel/stride	#filters	Pooling
3D Conv 1	(3, 3, 1)/1	64	(2, 2, 2)
3D Conv 2	(3, 3, 1)/2	128	(2, 2, 2)
3D Conv 3	(5, 5, 3)/1	64	(2, 2, 1)
3D Conv 4	(5, 5, 1)/2	32	(2, 2, 1)

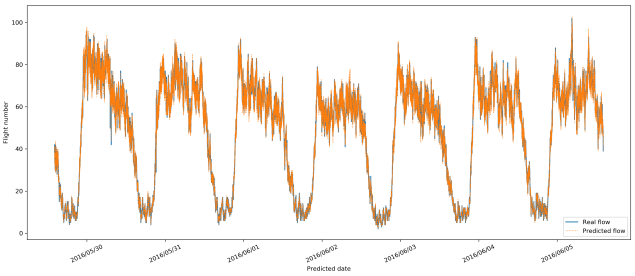

FIGURE 5. The predicted traffic flow for JHR.

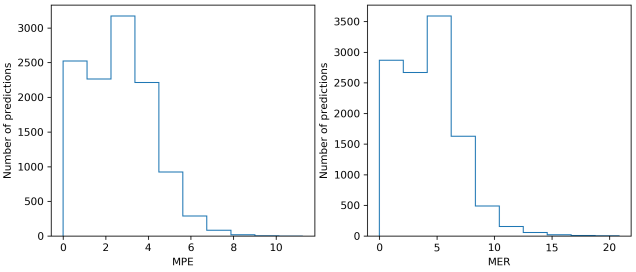

FIGURE 6. The histogram of the prediction error (MPE and MER) for JHR.

A single TSG is finally encoded as a feature vector with 2560-dimension. The feature vector is further fed into a LSTM layer with 1024 hidden units to mine the temporal dependencies of air traffic flow. Finally, a fully connected predicting layer is designed to estimate the traffic flow for the studied airspaces.

Based on the optimized parameters, the final training and prediction experiments are conducted to evaluate the performance of the proposed model. In those experiments, the total traffic flow, flight level distribution and the error ratio of the studied airspaces are applied to make comparison with real data in this week. In this section, experimental results are also discussed to explain the frequent patterns of air traffic flow.

Fig.5-10 show the experimental results for evaluating the performance of the proposed model. Fig.5 and Fig.8 show the predicted traffic flow and real traffic flow (true values) of the JHR and JGR in the test dataset, respectively. Fig.6 and Fig.9 show the prediction error of the JHR and JGR respectively, in which both the MPE and MER are reported as histograms. Fig.7 and Fig.10 show the traffic flow distribution on different flight levels (the predicted and real traffic flow) for the JHR and JGR, respectively.

From the figures, we can see that the predicted traffic flow for the studied airspaces on given days are closed to their

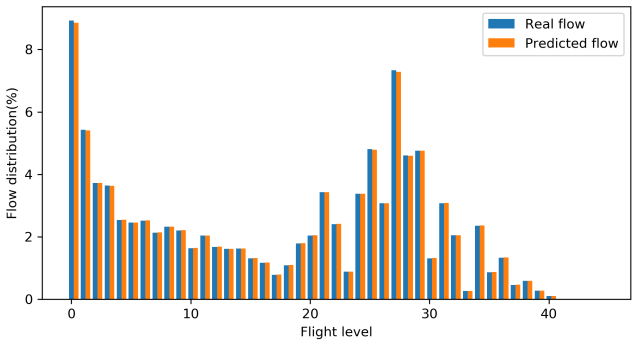

FIGURE 7. Traffic flow distribution on different flight levels for JHR.

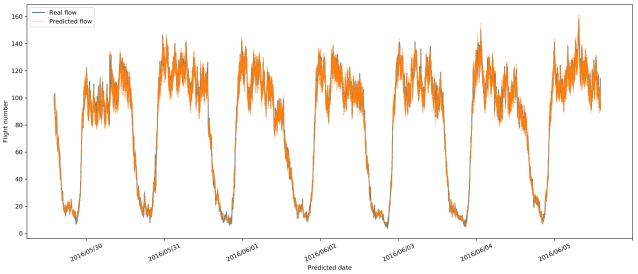

FIGURE 8. The predicted traffic flow for JGR.

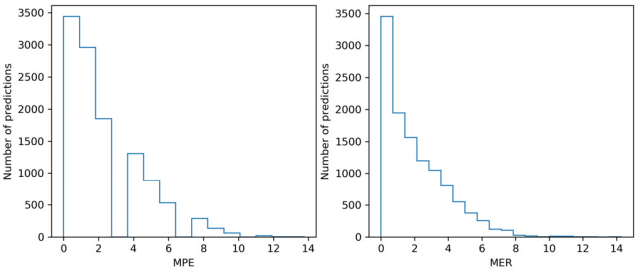

FIGURE 9. The histogram of the prediction error (MPE and MER) for JGR.

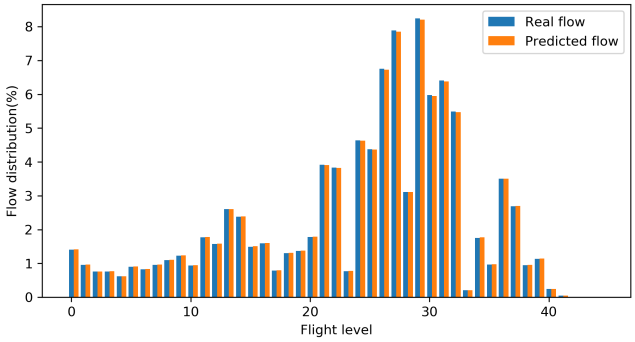

FIGURE 10. Traffic flow distribution on different flight levels for JGR.

collected traffic flow (true values), which proves the accuracy and robustness of the proposed model. In addition, we also come to the following understandings below based on the analysis of experimental results:

a) The traffic flow of the JHR at May 30, 2016 is busier than that of other days in this week obviously. By checking the real-time influences, we find that there is a routine event near this route, so more flights are required to meet the transportation demands. The experimental results indicate that the proposed model is able to consider the real-time impacts for predicting the air traffic flow by the proposed new data representation, i.e., TSG.
b) The traffic flow of both the JHR and JGR shows huge fluctuation from 9 am to 18.pm. Since both the two airspaces are trunk route in China, most flights will pass the studied routes in the near areas. The traffic flow patterns of a trunk route show a frequent flow-splitting and convergence in the concerned areas. This is a strong proof that the proposed model takes the general temporal dependencies of air traffic flow tendency.
c) As can be seen from the figure, more traffic flow of the JHR distributes in the low flight levels. It is easy to know that there are two civil airports in Shanghai, which concentrates more flight departure and landing in this studied area. Meanwhile, Shanghai is a main transfer airport for international flights outside China, which is denoted by the traffic flow distribution on flight levels. It is believed that spatial patterns of air traffic system are captured by the proposed model for predicting air traffic flow. Similarly, the traffic flow of the JGR distributes in the cruise altitude, from flight level 20 to 30, due to its spatial location in the studied airspace.
d) The prediction errors (MPE and MER) show a different trend for the studied airspaces. The prediction error of the JHR spread in a wide range, which attributes to the flight departure and landing in this route. The aircraft has higher maneuverability during flight departure and landing, which aggravates the nonlinearity of the traffic flow patterns and further reduces the prediction accuracy. The MPE and MER of the JGR are in low prediction errors since most flights are in cruise phase in this route.

To further show performance of the proposed model, more experiments are designed as the comparison baselines, including FTP, RP, and NN (specifically the FC-NN, B-LSTM, FC-NN+LSTM and 2D-CNN+LSTM based models). The experimental results are reported in Tab.3. In this section, only the total traffic flow of the studied airspaces (without flight level distributions) is predicted and evaluated by the proposed measurements. The listed results are the best one of different models during the experiments.

According to the result, we can see that the proposed model shows the desired superior performance over the designed baselines. The experimental result can be summarized as follows:

a) The FTP based ATFP approach is a bottom-up one, in which the ATFP is implemented based on the FTP. Therefore, the ATFP results are heavily influenced by the FTP performance, and the prediction error of the FTP limits the ATFP accuracy. As can be seen from result, the FTP based ATFP approach suffers the largest prediction error (MPE and MER) in the listed methods. In this work, the customized airspace generated by the TSG are refined ones with smaller spatial extent. Therefore, the influence of FTP errors for the flight in the airspace margin on the ATFP accuracy is frequent and hugely magnified. Besides, the FTP accuracy in the cruise phase is higher than that of in the cruise/descent phase, which will cause larger deviation of the prediction results, as shown as the PEV in the result.
b) The results obtained by the FC-NN model also has large deviation with the ground truth. Since the FC-NN cannot consider the temporal and spatial dependencies for predicting the air traffic flow jointly (mainly focuses spatial dependencies in the experiment), it fails to obtain a comparable performance with other models.
c) In general, all the following methods, regression, B-LSTM, and FC-NN+LSTM model, are based on the time series processing algorithms. The regression mainly considers the temporal dependencies of air traffic flow, which finally predict the traffic flow with larger prediction error (10.71 and 9.41%). The LSTM based models consider the temporal dependencies and minor spatial dependencies by organizing the input as a traffic flow vector. Therefore, the LSTM based approaches has the ability of obtaining higher prediction performance (MPE, MER, PEV) than that of the first three baselines due to the powerful ability of modeling nonlinearity. By improving the model capacity and its representation ability on nonlinear features, the FC-NN+LSTM model can obtain better results than that of B-LSTM model.
d) Finally, the 2D-CNN+LSTM based model is designed to prove the validity on predicting the distribution on flight levels by extending the 2D-CNN to 3D-CNN. In the two experiments, the TSG is well organized by considering the spatial dependencies and LSTM block is designed to mine the temporal dependencies. The prediction results really show the desired improvement since the 3D specificity is the key to capture the transition patterns in the air traffic system.

TABLE 3. Comparison of prediction with different approaches.

Category	Approaches	MPE	MER (%)	PEV
FTP	FTP	11.99	9.74	17.54
RP	Regression	10.71	9.41	9.55
NN	FC-NN	11.55	9.60	14.69
	B-LSTM	9.68	9.24	11.33
	FC-NN+LSTM	7.90	7.54	8.20
	2D-CNN+LSTM	6.05	5.91	6.24
	R-3DCNN*	5.67	5.25	5.97

In addition, we also compare the mean error of flight level distribution (0.15% of R-3DCNN versus 0.36% of 2D-CNN+LSTM) to show the advantage of 3D-CNN on predicting the traffic flow on flight level distribution.

In summary, based on the experimental results, the proposed model shows higher accuracy and stability of the prediction results among all the comparison baselines, and the traffic flow distribution on different flight levels show the same trend. The proposed TSG illustrates required spatial patterns on a single input, which promotes the modeling performance in this work. The LSTM layer is further proposed to build the temporal patterns of traffic flow, which integrates the spatial and temporal information for air traffic flow prediction comprehensively.

VI. CONCLUSION

Air traffic is a complex and time-varying system and easy to be influenced by real-time factors. To overcome the low predicting accuracy and stability of existing methods on the air traffic flow prediction, a deep neural network (R-3DCNN) based air traffic flow prediction approach is proposed in this paper. A data representation called TSG is firstly proposed to integrate the model input and describe the spatial dependencies of air traffic situation. The TSG illustrates the spatial dependencies of air traffic flow on adjacent areas and flight levels, which is essential to the ATFP research. Meanwhile, real-time factors, such as important activities, adverse weather, etc., can also be represented on the TSG. Naturally, 3D-CNN layers are applied to mine high-level abstract features of air traffic flow by the convolutional operations. A LSTM layer is also designed to build the temporal dependencies of air traffic flow, i.e., the historical TSG sequence. The accuracy, stability and robustness superiority of the proposed model is fully proved by several designed experiments with real data. Comparison experimental results with other baseline models are also obtained to validate the proposed model. Besides, the improvement of the proposed data representation, i.e., the TSG for representing the spatial dependencies and real-time factors, is also confirmed by the 2D-CNN and 3D-CNN based experiments, respectively.

In the future, we will apply the improvement of ATFP to real air traffic management scene. Based on the proposed approach and combining it with the theory of traffic scheduling, a refined air traffic management system with more efficient and effective joint operation and controlling measures are expected to fulfill in busiest areas in China. That's what we want to do for solving facing problems of the civil aviation in China.

REFERENCES

[1] A. M. Bayen, P. Grieder, and C. Tomlin, "A control theoretic predictive model for sector-based air traffic flow," in *Proc. AIAA Guid., Navigat., Control Conf. Exhibit*, Aug. 2002, p. 5011.

[2] A. Black, "The chicago area transportation study: A case study of rational planning," *J. Planning Educ. Res.*, vol. 10, no. 1, pp. 27–37, Oct. 1990.

[3] E. Ko, J. Ahn, and E. Y. Kim, "3D Markov process for traffic flow prediction in real-time," *Sensors*, vol. 16, no. 2, p. 147, 2016.

[4] Z. Ma, G. Luo, and D. Huang, "Short term traffic flow prediction based on on-line sequential extreme learning machine," in *Proc. 8th Int. Conf. Adv. Comput. Intell., (ICACI)*, Feb. 2016, pp. 143–149.

[5] Q. Shang, C. Lin, Z. Yang, Q. Bing, and X. Zhou, "A hybrid short-term traffic flow prediction model based on singular spectrum analysis and kernel extreme learning machine," *PLoS One*, vol. 11, no. 8, Aug. 2016, Art. no. e0161259.

[6] C. Chen, J. Hu, Q. Meng, and Y. Zhang, "Short-time traffic flow prediction with ARIMA-GARCH model," in *Proc. IEEE Intell. Vehicles Symp.*, Jun. 2011, pp. 607–612.

[7] A. Pascale and M. Nicoli, "Adaptive Bayesian network for traffic flow prediction," in *Proc. IEEE Stat. Signal Process. Workshop (SSP)*, Jun. 2011, pp. 177–180.

[8] M. Castro-Neto, Y.-S. Jeong, M.-K. Jeong, and L. D. Han, "Online-SVR for short-term traffic flow prediction under typical and atypical traffic conditions," *Expert Syst. Appl.*, vol. 36, no. 3, pp. 6164–6173, 2009.

[9] Y. Lv, Y. Duan, W. Kang, Z. Li, and F.-Y. Wang, "Traffic flow prediction with big data: A deep learning approach," *IEEE Trans. Intell. Transp. Syst.*, vol. 16, no. 2, pp. 865–873, Apr. 2015.

[10] A. Sladkowski and W. Pamuła, *Intelligent Transportation Systems-Problems and Perspectives*, vol. 303. Berlin, Germany: Springer, 2016.

[11] D. Cui, S. Wu, and B. Xu, "Air traffic flow forecasts based on artificial neural networks combined with regression methods," *Qinghua Daxue Xuebao/J. Tsinghua Univ.*, vol. 45, no. 1, pp. 96–99, Jan. 2005.

[12] M. Zhang, S. Han, and L. Huang, "Air traffic flow combinational forecast based on double gravity model and artificial neural network," *J. Southwest Jiaotong Univ.*, vol. 8, no. 2, pp. 4–5, 2009.

[13] F. Qiu and Y. Li, "Air traffic flow of genetic algorithm to optimize wavelet neural network prediction," in *Proc. 5th Int. Conf. Softw. Eng. Service Sci.*, Jun. 2014, pp. 1162–1165.

[14] F. Yao, "Research on flight traffic assignment of route network based on DSO," *J. Binzhou Univ.*, vol. 32, no. 2, pp. 15–19, 2016.

[15] D. Bertsimas and S. Gupta, "Fairness and collaboration in network air traffic flow management: An optimization approach," *Transp. Sci.*, vol. 50, no. 1, pp. 57–76, 2016.

[16] Q. Li, Y. Zhang, and R. Su, "A flow-based flight scheduler for en-route air traffic management," *IFAC-PapersOnLine*, vol. 49, no. 3, pp. 353–358, 2016.

[17] T. Cheng, D. Cui, and P. Cheng, "Data mining for air traffic flow forecasting: A hybrid model of neural network and statistical analysis," in *Proc. IEEE Int. Conf. Intell. Transp. Syst.*, vol. 1, Oct. 2003, pp. 211–215.

[18] Y. Cao, L. Zhang, and D. Sun, An air traffic prediction model based on kernel density estimation. in *Proc. Amer. Control Conf.*, Jun. 2013, pp. 6333–6338.

[19] Z. Sun, Z. Li, and Y. Zhao, "Traffic congestion forecasting based on possibility theory," *Int. J. Intell. Transp. Syst. Res.*, vol. 14, no. 2, pp. 85–91, May 2016.

[20] H. Zhang, C.-P. Jiang, and L. Yang, "Forecasting traffic congestion status in terminal areas based on support vector machine," *Adv. Mech. Eng.*, vol. 8, no. 9, Sep. 2016, Art. no. 168781401666738.

[21] S. Chen, "Short-term air traffic flow prediction based on run-time data of Eurocat-X system," *Inf. Commun.*, vol. 5, pp. 42–44, Aug. 2013.

[22] Z. Lu and T. Wang, "Air traffic flow prediction based on least squares support vector regression," *Energy Procedia*, vol. 11, pp. 947–951, Jan. 2011.

[23] S. Ren, K. He, R. Girshick, and J. Sun, "Faster R-CNN: Towards real-time object detection with region proposal networks," *IEEE Trans. Pattern Anal. Mach. Intell.*, vol. 39, no. 6, pp. 1137–1149, Jun. 2017.

[24] K. Simonyan and A. Zisserman, "Two-stream convolutional networks for action recognition in videos," in *Proc. Adv. Neural Inf. Process. Syst.*, Jun. 2014, pp. 568–576.

[25] J. Donahue, L. A. Hendricks, S. Guadarrama, M. Rohrbach, S. Venugopalan, K. Saenko, and T. Darrell, "Long-term recurrent convolutional networks for visual recognition and description," *IEEE Trans. Pattern Anal. Mach. Intell.*, vol. 39, no. 4, pp. 677–691, Apr. 2017.

[26] S. Ji, W. Xu, M. Yang, and K. Yu, "3D convolutional neural networks for human action recognition," *IEEE Trans. Pattern Anal. Mach. Intell.*, vol. 35, no. 1, pp. 221–231, Jan. 2013.

[27] M. Baccouche, F. Mamalet, C. Wolf, C. Garcia, and A. Baskurt, "Sequential deep learning for human action recognition," in *Proc. Int. Workshop Hum. Behav. Understand.*, 2011, pp. 29–39.

[28] S. Lai, L. Xu, K. Liu, and J. Zhao, "Recurrent convolutional neural networks for text classification," in *Proc. 29th AAAI Conf. Artif. Intell.*, Feb. 2015, pp. 2267–2273.

[29] P. O. Pinheiro and R. Collobert, "Recurrent convolutional neural networks for scene labeling," in *Proc. 31st Int. Conf. Int. Conf. Mach. Learn.*, vol. 32, 2014, pp. 82–90.
[30] X.-P. Wu, H.-Y. Yang, and S.-C. Han, "Analysis on network properties of multivariate mixed air traffic management technical support system based on complex network theory," *Acta Phys. Sinica*, vol. 65, no. 14, pp. 15–23, Jul. 2016.
[31] W. J. Zhang, S. Y. Wang, and Y. L. Feng, "Huber-based high-degree cubature Kalman tracking algorithm," *Acta Phys. Sinica*, vol. 65, no. 8, pp. 354–362, 2016.
[32] T. W. M. Vossen, R. Hoffman, and A. Mukherjee, "Air traffic flow management," in *Quantitative Problem Solving Methods in the Airline Industry: A Modeling Methodology Handbook*. Berlin, Germany: Springer, 2012, pp. 385–453.
[33] Y. LeCun and Y. Bengio, "Convolutional networks for images, speech, and time series," in *The Handbook of Brain Theory and Neural Networks*, M. A. Arbib, Ed. Cambridge, MA, USA: MIT Press, 1995, pp. 255–258.
[34] Z. Zuo, B. Shuai, G. Wang, X. Liu, X. Wang, B. Wang, and Y. Chen, "Convolutional recurrent neural networks: Learning spatial dependencies for image representation," in *Proc. IEEE Conf. Comput. Vis. Pattern Recognit. Workshops (CVPRW)*, Jun. 2015, pp. 18–26.
[35] G. Trigeorgis, F. Ringeval, R. Brueckner, E. Marchi, M. A. Nicolaou, B. Schuller, and S. Zafeiriou, "Adieu features? End-to-end speech emotion recognition using a deep convolutional recurrent network," in *Proc. IEEE Int. Conf. Acoust., Speech Signal Process. (ICASSP)*, Mar. 2016, pp. 5200–5204.
[36] G. C. Cawley, N. L. Talbot, and M. Girolami, "Sparse multinomial logistic regression via Bayesian l1 regularisation," in *Proc. Adv. Neural Inf. Process. Syst.*, 2007, pp. 209–216.
[37] C. Sriram and A. Haghani, "An optimization model for aircraft maintenance scheduling and re-assignment," *Transp. Res. A, Policy Pract.*, vol. 37, no. 1, pp. 29–48, Jan. 2003.
[38] C. Xu, "Comparison and thought of three flight level system reforms of China," *China Civ. Aviat.*, vol. 12, no. 1, pp. 29–31, 2014.
[39] Y. Lin, J.-W. Zhang, and H. Liu, "An algorithm for trajectory prediction of flight plan based on relative motion between positions," *Frontiers Inf. Technol. Electron. Eng.*, vol. 19, no. 7, pp. 905–916, Jul. 2018.

HONG LIU received the Ph.D. degree from Sichuan University, Chengdu, China, in 2014, where he has been working for teaching and research work, since 2007. He has been an Associate Professor, since 2015. His research interests include air traffic management and real-time software engineering.

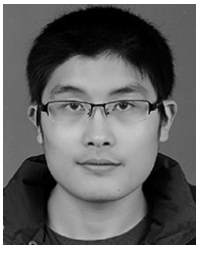

YI LIN received the Ph.D. degree from Sichuan University, Chengdu, China, in 2019, where he is currently an Assistant Professor. He is also a Visiting Scholar with the University of Wisconsin–Madison. His research interests include air traffic flow management, machine learning, and deep learning applications on air traffic management.

ZHENGMAO CHEN received the M.S. degree from Sichuan University, Chengdu, China, in 2003, where he began his teaching career. His research interests include digital signal processing, data fusion, and the development of the voice record system in air traffic control systems.

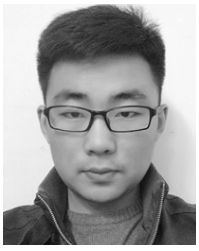

DONGYUE GUO received the B.E. degree in the telecommunication engineering from Yantai University, Yantai, China, in 2017. He is currently pursuing the M.S. degree with the National Key Laboratory of Fundamental Science on Synthetic Vision, Sichuan University, Chengdu, China. His research interests include the speech signal preprocessing.

JIANWEI ZHANG received the Ph.D. degree from Sichuan University, Chengdu, China, in 2008, where he has been working for teaching and research work, since 1993. He has published more than 30 articles. His research interests include air traffic management, and intelligent image analysis and processing. He received the National Science and Technology Progress Award.

HAILONG JING received the Ph.D. degree from Sichuan University, Chengdu, China, in 2017, where he is currently an Assistant Professor. His research interest includes the deep learning applications.